

Supporting information

High- χ Alternating Copolymers for Accessing Sub-5 nm Domains *via* Simulations

Shanlong Li, Qingsong Xu, Ke Li, Chunyang Yu, and Yongfeng Zhou**

School of Chemistry & Chemical Engineering, State Key Laboratory of Metal Matrix Composites, Shanghai Key Laboratory of Electrical Insulation and Thermal Aging, Shanghai Jiao Tong University, 800 Dongchuan Road, Shanghai, 200240, China

- S1. Construction of coarse-grained model.**
- S2. Validation of the force field and CG model.**
- S3. Simulation details.**
- S4. Justification of simulation time.**
- S5. The calculation of the structure factors.**
- S6. The sizes of polar and apolar domains in lamellae and cylinders.**
- S7. The definition of packing parameters of repeating units of ACPs.**
- S8. The calculation of asphericity of polymer chains.**
- S9. The effect of molecular weight.**
- S10. Glass transition temperature.**
- S11. Polydisperse systems.**
- S12. References.**

S1. Construction of coarse-grained model.

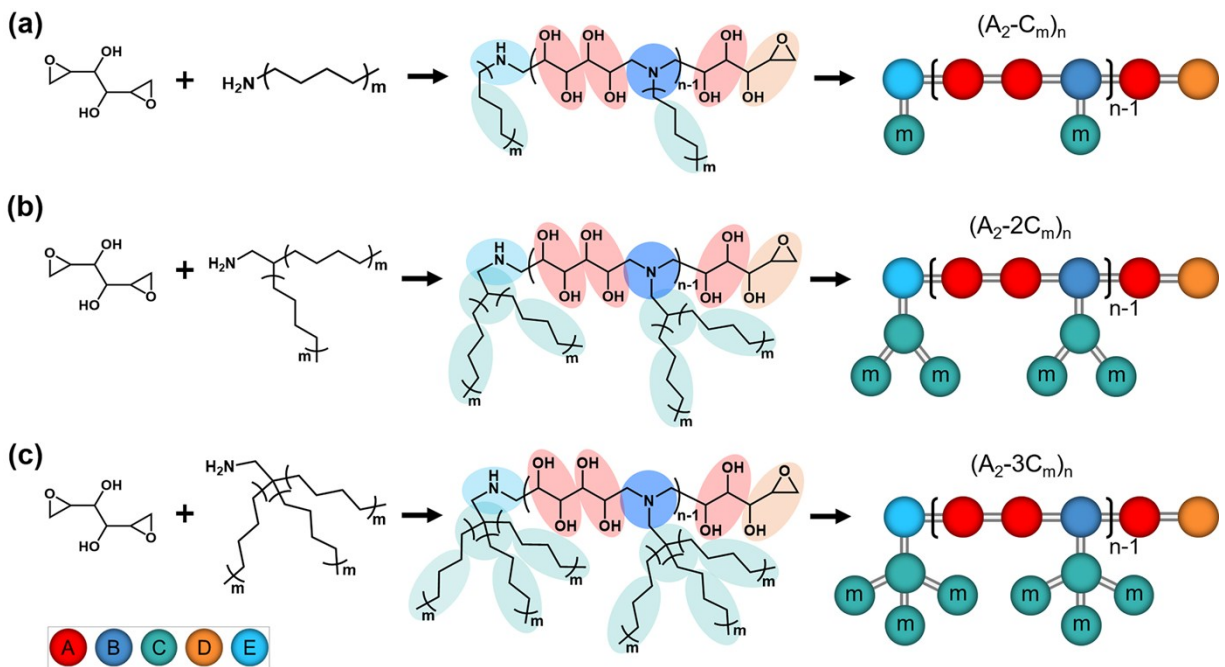
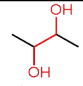
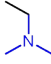
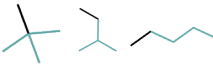
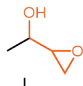
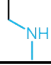


Fig. S1 The synthesis and coarse-grained mapping of ACPs with different alkyl chains. Different chemical groups are scaled into CG beads A, B, C, D and E, which are red, blue, cyan, orange and light blue, respectively. The CG models are named as $(A_2-C_m)_n$, $(A_2-2C_m)_n$ and $(A_2-3C_m)_n$ for the ACPs with one (a), two (b) and three (c) armed alkyl chains, respectively. m and n represent the length of alkyl chain and degree of polymerization, respectively.

Table S1. Bead types and self-interaction parameters used in the simulations.

groups	bead name	bead type	σ (nm)	ϵ (kJ/mol)
	A	P ₄	0.47	5.0
	B	N ₀	0.47	3.5
	C	C ₁	0.47	3.5
	D	P ₂	0.47	4.5
	E	SN _{da}	0.43	3.375

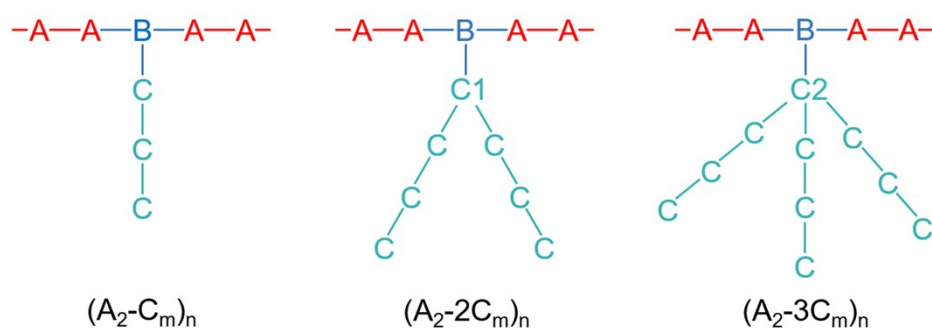


Fig. S2 Molecular structure to clarify the bonded terms in the CG models of ACPs.

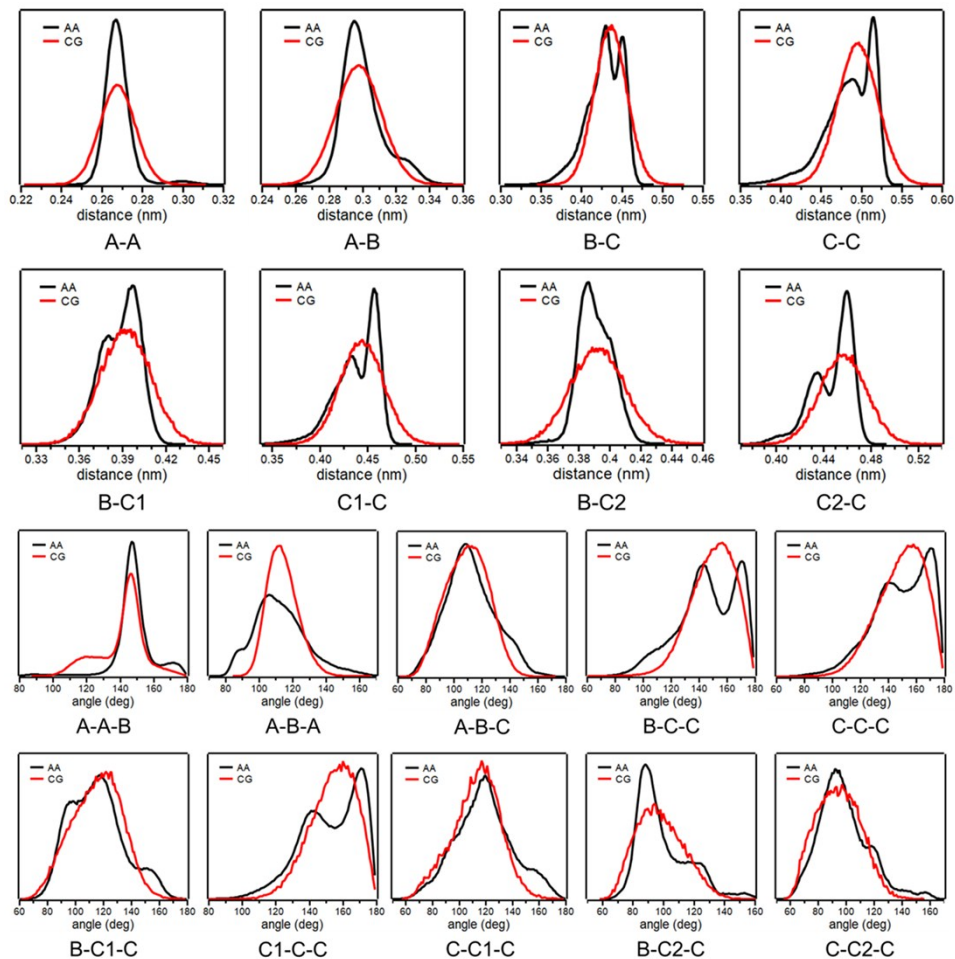


Fig. S3 Distributions of bonded terms from both AA and CG simulations. Distributions from atomistic GAFF simulations are in dark, and CG Martini distributions are in red. The captions of the terms are corresponding to Fig. S2.

Table S2. Bonded parameters used in the simulations.

bond	b_0 (nm)	k_b (kJ·mol ⁻¹ ·nm ⁻²)	angle	θ_0 (deg)	k_θ (kJ·mol ⁻¹ ·rad ⁻²)
A-A	0.27	40000	A-A-B	147.0	300.0
A-B	0.30	16000	A-B-A	100.0	50.0
B-C	0.44	10000	A-B-C/C1/C2	105.0	40.0
C-C	0.50	10000	B-C-C	175.0	15.0
B-C1	0.40	10000	C-C-C	175.0	20.0
C1-C	0.45	6000	B-C1-C	120.0	25.0
B-C2	0.40	10000	C1/C2-C-C	175.0	25.0
C2-C	0.46	8000	C-C1-C	125.0	25.0
			B-C2-C	95.0	40.0
			C-C2-C	100.0	50.0

S2. Validation of the force field and CG model.

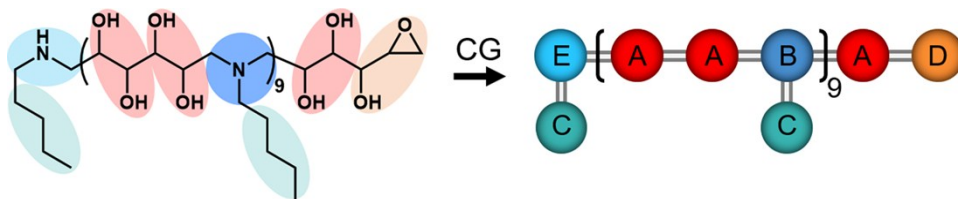


Fig. S4 Atomistic and CG models of $(A_2-C_1)_{10}$ for force field validation.

Table S3. The values of density (ρ), radius of gyration (R_g) and end-to-end distance (R_e) of ACP in the melt from both AA and CG simulations.

simulation	ρ (kg/m ³)	R_g (nm)	R_e (nm)
AA	1030 \pm 6	1.23 \pm 0.01	3.28 \pm 0.07
CG	1027 \pm 5	1.21 \pm 0.02	3.05 \pm 0.09

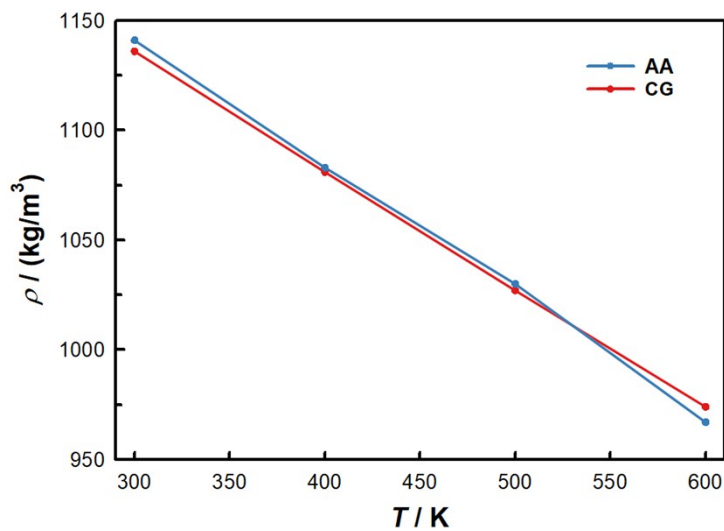


Fig. S5 Temperature dependence of the density for the atomistic and CG models.

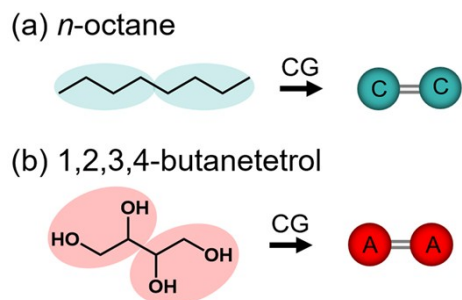


Fig. S6 Atomistic and CG models of *n*-octane (a) and 1,2,3,4-butanetetrol (b).

Table S4. The values of solubility parameters of *n*-octane and 1,2,3,4-butanetetrol from both AA and CG simulations.

molecules	δ_{CG} (cal ^{1/2} /cm ^{3/2})	δ_{AA} (cal ^{1/2} /cm ^{3/2})	δ_{HSP}^* (cal ^{1/2} /cm ^{3/2})	δ_{exp} (cal ^{1/2} /cm ^{3/2})
<i>n</i> -octane	6.63 ₂	7.52 ₉	7.55 ₂	7.55
1,2,3,4- butanetetrol	16.15 ₄	18.39 ₆	19.65 ₄	-

* δ_{HSP} is the compositive value of Hansen solubility parameters predicted according to the group contributions to partial solubility parameters.¹

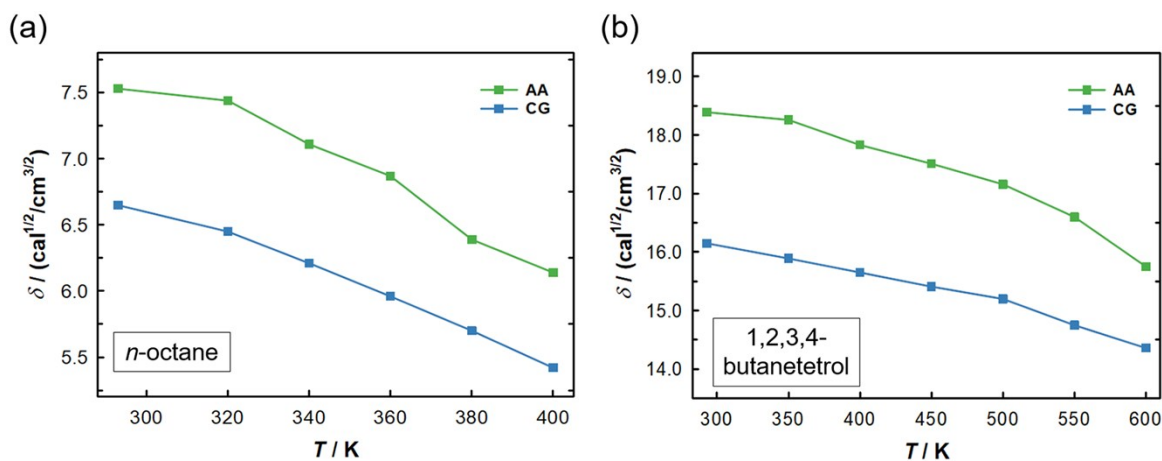


Fig. S7 Temperature dependence of the solubility parameters (δ) of *n*-octane (a) and 1,2,3,4-butanetetrol (b) obtained from both AA and CG simulations.

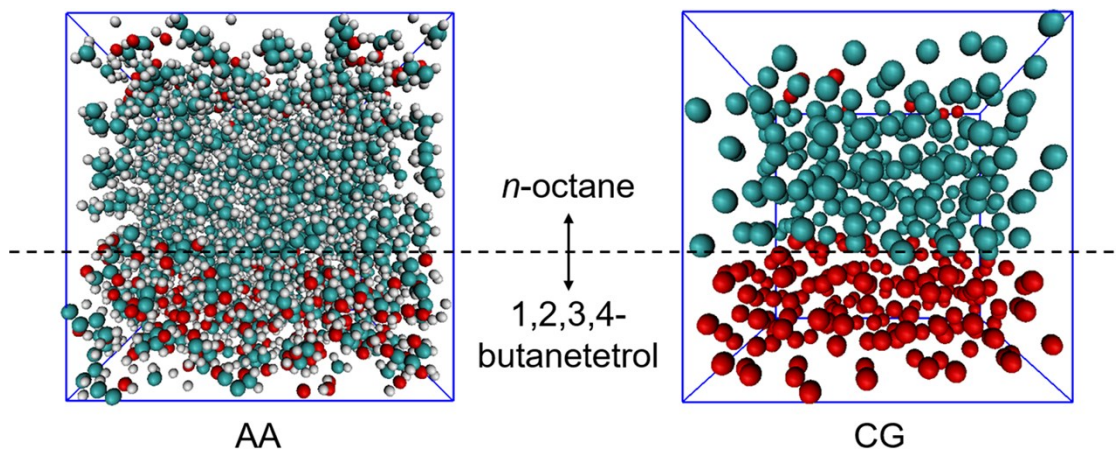


Fig. S8 The phase separation of *n*-octane and 1,2,3,4-butanetetrol in both AA and CG simulations.

S3. Simulation details.

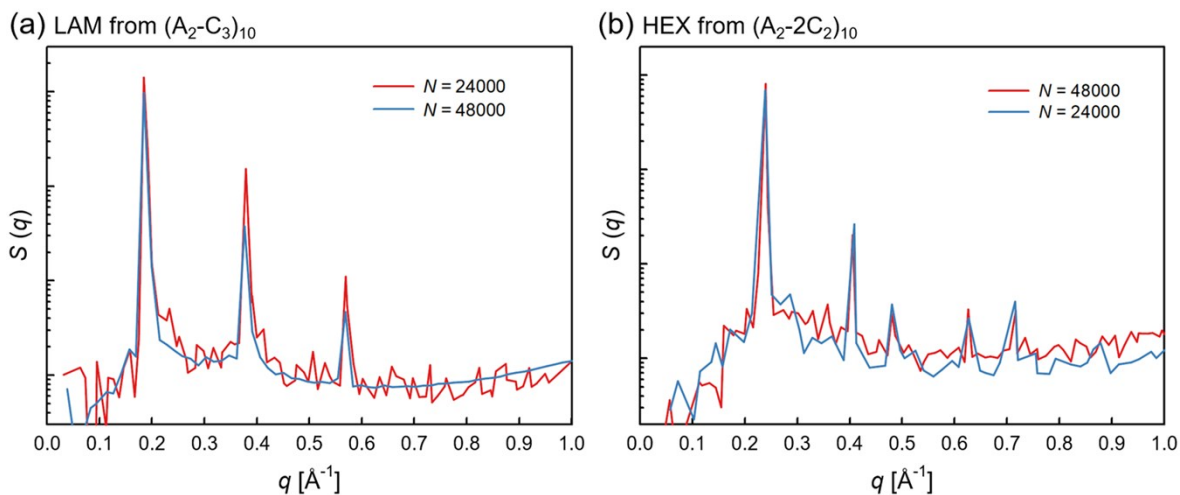


Fig. S9 Structure factors of LAM (a) and HEX (b) obtained from polymer $(A_2-C_3)_{10}$ and $(A_2-2C_2)_{10}$, for different system sizes.

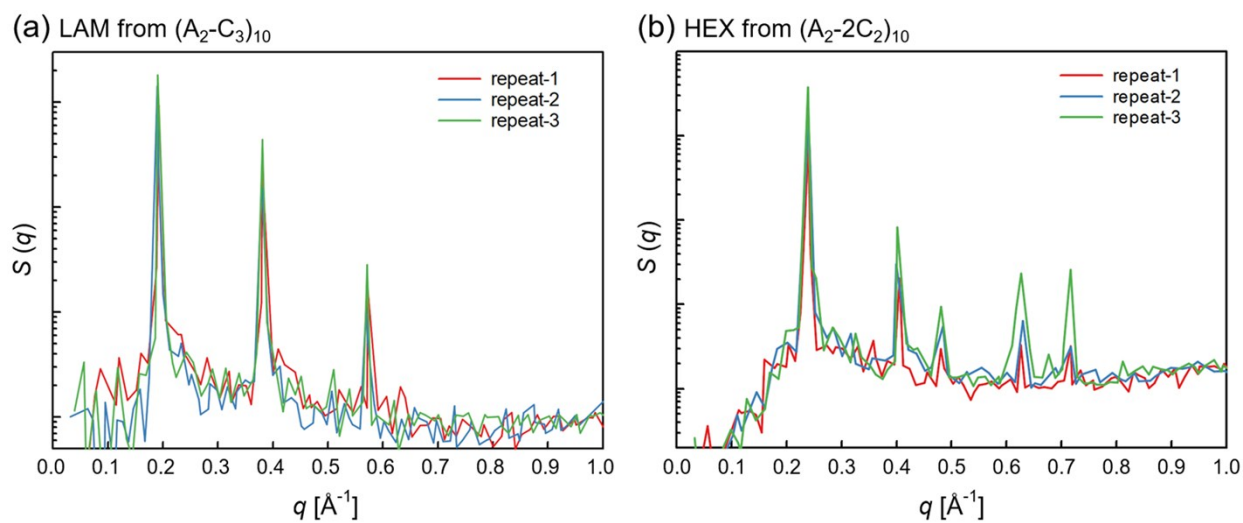


Fig. S10 Structure factors from three independent simulations of LAM (a) and HEX (b) obtained from polymer $(A_2-C_3)_{10}$ and $(A_2-2C_2)_{10}$.

Table S5. The order-to-disorder transition temperatures (T_{ODT}) of different polymers.

polymer	T_{ODT} (K)	polymer	T_{ODT} (K)
$(\text{A}_2\text{-C}_1)_{10}$	-	$(\text{A}_2\text{-2C}_1)_{10}$	580
$(\text{A}_2\text{-C}_2)_{10}$	650	$(\text{A}_2\text{-2C}_2)_{10}$	640
$(\text{A}_2\text{-C}_3)_{10}$	685	$(\text{A}_2\text{-2C}_3)_{10}$	680
$(\text{A}_2\text{-C}_4)_{10}$	710	$(\text{A}_2\text{-3C}_1)_{10}$	570
$(\text{A}_2\text{-C}_5)_{10}$	730	$(\text{A}_2\text{-3C}_2)_{10}$	650

S4. Justification of simulation time.

The diffusion coefficient (D) was defined through the Einstein equation

$$6Dt = \lim_{t \rightarrow \infty} \langle |\vec{r}(t) - \vec{r}(0)|^2 \rangle$$

Thus, D can be calculated through the mean square displacement (MSD) of polymer chains.

Table S6. Diffusion coefficient (D), the average distance one chain moves in 1.2 us (d_{move}), the radius of gyration of the chain (R_g), and the ratio between d_{move} and R_g at 753K.

Polymers	D (cm ² /s)	d_{move} (nm)	R_g (nm)	d_{move}/R_g
(A ₂ -C ₅) ₁₅	$4.58 (\pm 0.61) \times 10^{-8}$	5.74 ± 0.38	1.91 ± 0.01	3.01
(A ₂ -2C ₃) ₁₅	$5.92 (\pm 0.59) \times 10^{-8}$	6.53 ± 0.33	1.83 ± 0.02	3.57
(A ₂ -3C ₂) ₁₅	$3.29 (\pm 0.46) \times 10^{-7}$	15.39 ± 1.08	1.42 ± 0.06	10.84

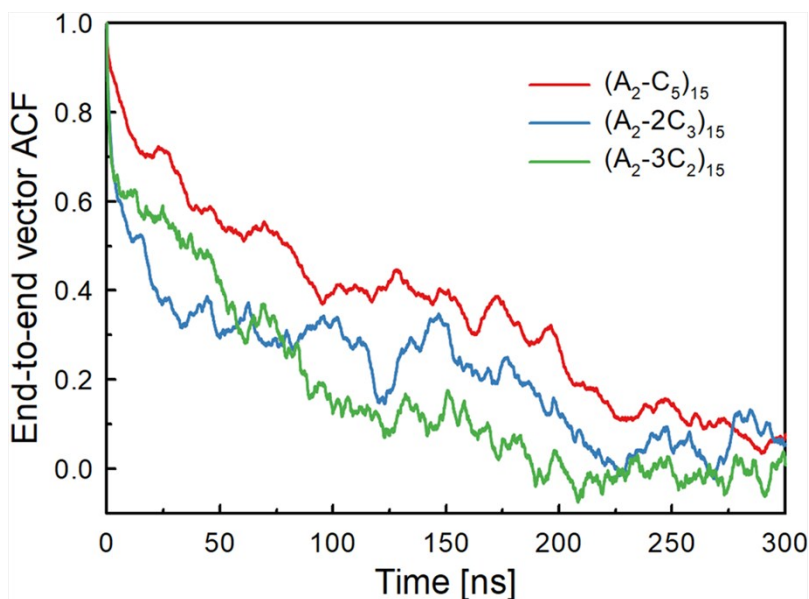


Fig. S11 The end-to-end vector autocorrelation function (ACF) for (A₂-C₅)₁₅, (A₂-2C₃)₁₅ and (A₂-3C₂)₁₅.

S5. The calculation of the structure factors.

According to the mathematical relationship between the simulation particle positions and structure factors $S(\mathbf{q})$, $S(\mathbf{q})$ can be calculated by using the following equation²

$$S(q) = \frac{\left(\sum_j \cos(q \cdot r_j)\right)^2 + \left(\sum_j \sin(q \cdot r_j)\right)^2}{N}$$

where \mathbf{q} is the wave vector, \mathbf{r}_j is the position of particle j , and N is the number of particles. \mathbf{q} is restricted to an integer number of wavelengths within the simulation box, which can be set as³

$$q = \frac{2\pi}{L_x}n_x e_x + \frac{2\pi}{L_y}n_y e_y + \frac{2\pi}{L_z}n_z e_z$$

where L_x , L_y and L_z are the box length at x , y and z dimensions, respectively. n_x , n_y and n_z are any integer number, except $n_x = n_y = n_z = 0$. e_x , e_y and e_z are the basis vectors in three dimensions.

Domain period d can be calculated from the peak position in the pattern of structure factors according to the relationship $d = 2\pi/q^*$, where q^* is the characteristic peak position. For lamellae, d is equal to the center-to-center distance of the lamellae, while d is the 100 interplanar distance for HEX. The center-to-center distance (L) of cylinders in HEX can be calculated through the

relationship $d = \frac{\sqrt{3}}{2}L$.

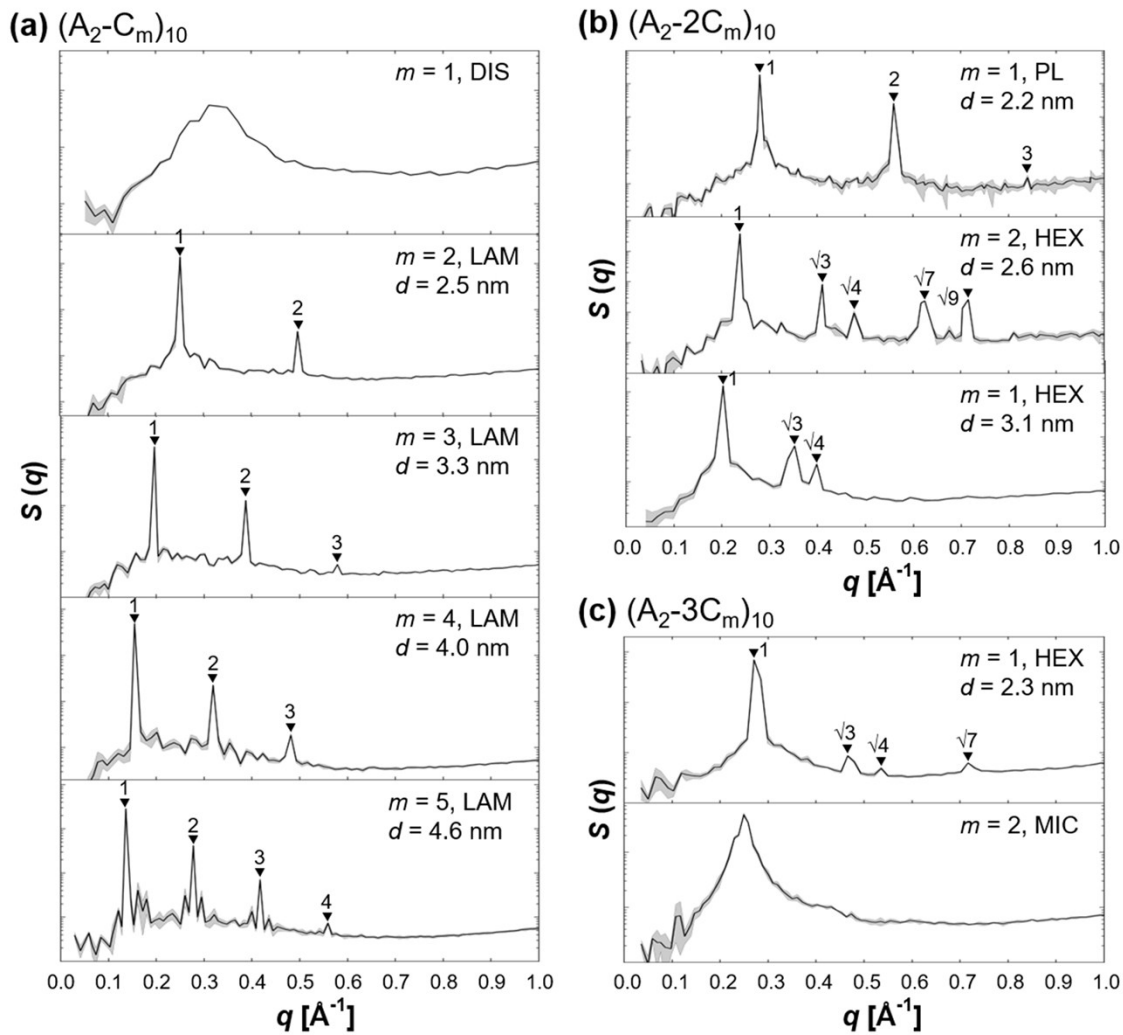


Fig. S12 Structure factors of the mesophases at 303K obtained from polymer $(A_2-C_m)_n$, $(A_2-2C_m)_n$, and $(A_2-3C_m)_n$, respectively. The legends indicate the values of m , the corresponding morphologies and domain periods d . The error bar is indicated as shadow of the curve. The peak positions (q) are labelled by the arrow symbols together with the value of q/q^* .

S6. The sizes of polar and apolar domains in lamellae and cylinders.

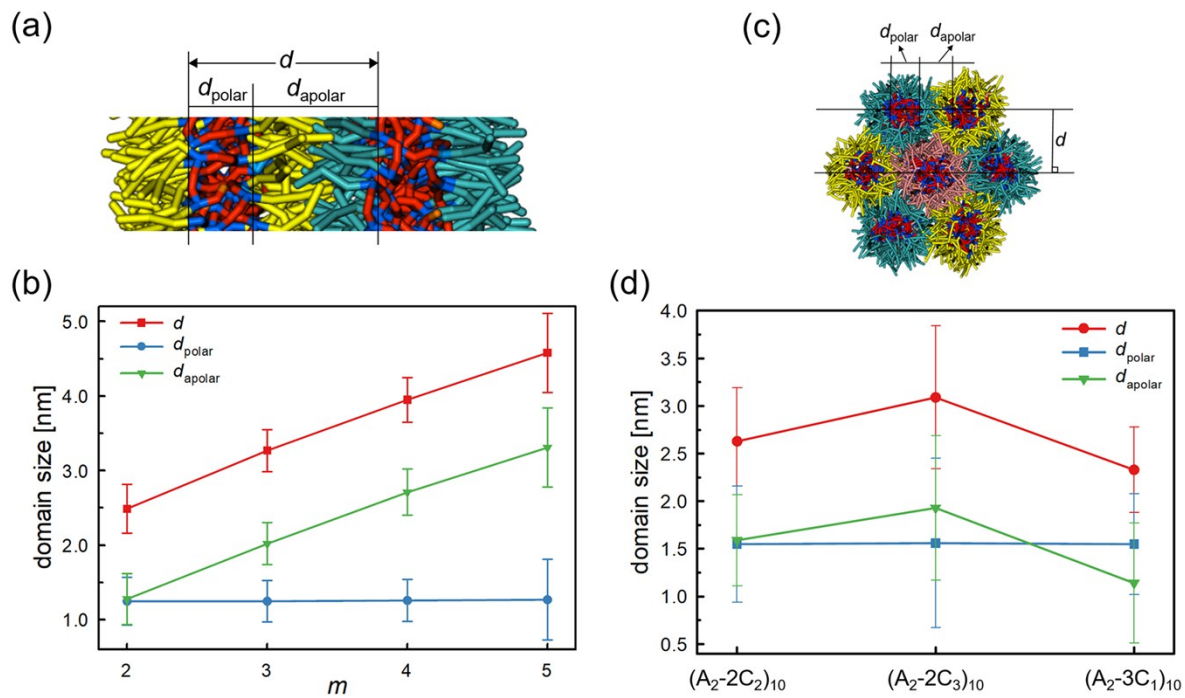


Fig. S13 Scheme for the definition (a, c) and the variation of d , d_{polar} and d_{apolar} with the increase of m in lamellae and cylinders (b, d).

S7. The definition of packing parameters of repeating units of ACPs.

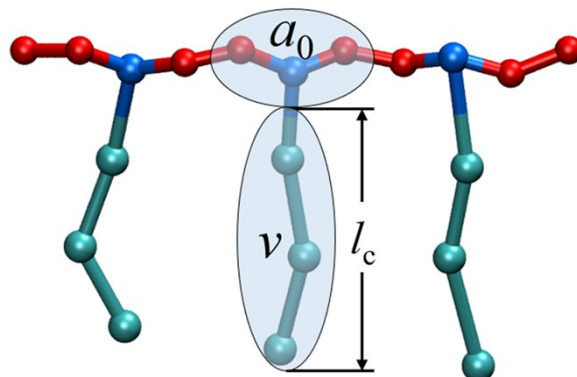


Fig. S14 Scheme for the definition of packing parameter of the ACPs.

Fig. S14 shows a part of the polymer chain, which is used to define the packing parameter (p) of ACPs. a_0 is the average area of the polar part of one repeating segment, while v and l_c are the volume and chain length of the apolar part of one repeating segment, respectively. Thus, packing parameter can be calculated by⁴

$$p = \frac{v}{a_0 l_c}$$

S8. The calculation of asphericity of polymer chains.

To measure the shape of polymer chains, the radius of gyration tensor is constructed,⁵⁻⁷

$$A = \begin{bmatrix} S_{xx} & S_{xy} & S_{xz} \\ S_{yx} & S_{yy} & S_{yz} \\ S_{zx} & S_{zy} & S_{zz} \end{bmatrix}$$

where each component can be calculated as

$$S_{xx} = \frac{1}{n} \sum_{i=1}^n (x_i - x_c)(x_i - x_c), S_{xy} = \frac{1}{n} \sum_{i=1}^n (x_i - x_c)(y_i - y_c), \dots$$

Thus, matrix A can be diagonalized to matrix S

$$S = \begin{bmatrix} \lambda_1^2 & 0 & 0 \\ 0 & \lambda_2^2 & 0 \\ 0 & 0 & \lambda_3^2 \end{bmatrix}$$

and the asphericity δ can be calculated via

$$\delta = \frac{(\lambda_1^2 - \lambda_2^2)^2 + (\lambda_2^2 - \lambda_3^2)^2 + (\lambda_3^2 - \lambda_1^2)^2}{2(\lambda_1^2 + \lambda_2^2 + \lambda_3^2)^2}$$

where δ takes the values $[0,1]$, and $\delta = 0$ represents for perfectly spherical globule, $\delta = 1$ for a rod, and $\delta = 0.25$ for a circle. Fig. S12 gives the values of asphericity (on the top of each column), mean square radius of gyration and its three components in X, Y and Z dimensions.

S9. The effect of molecular weight.

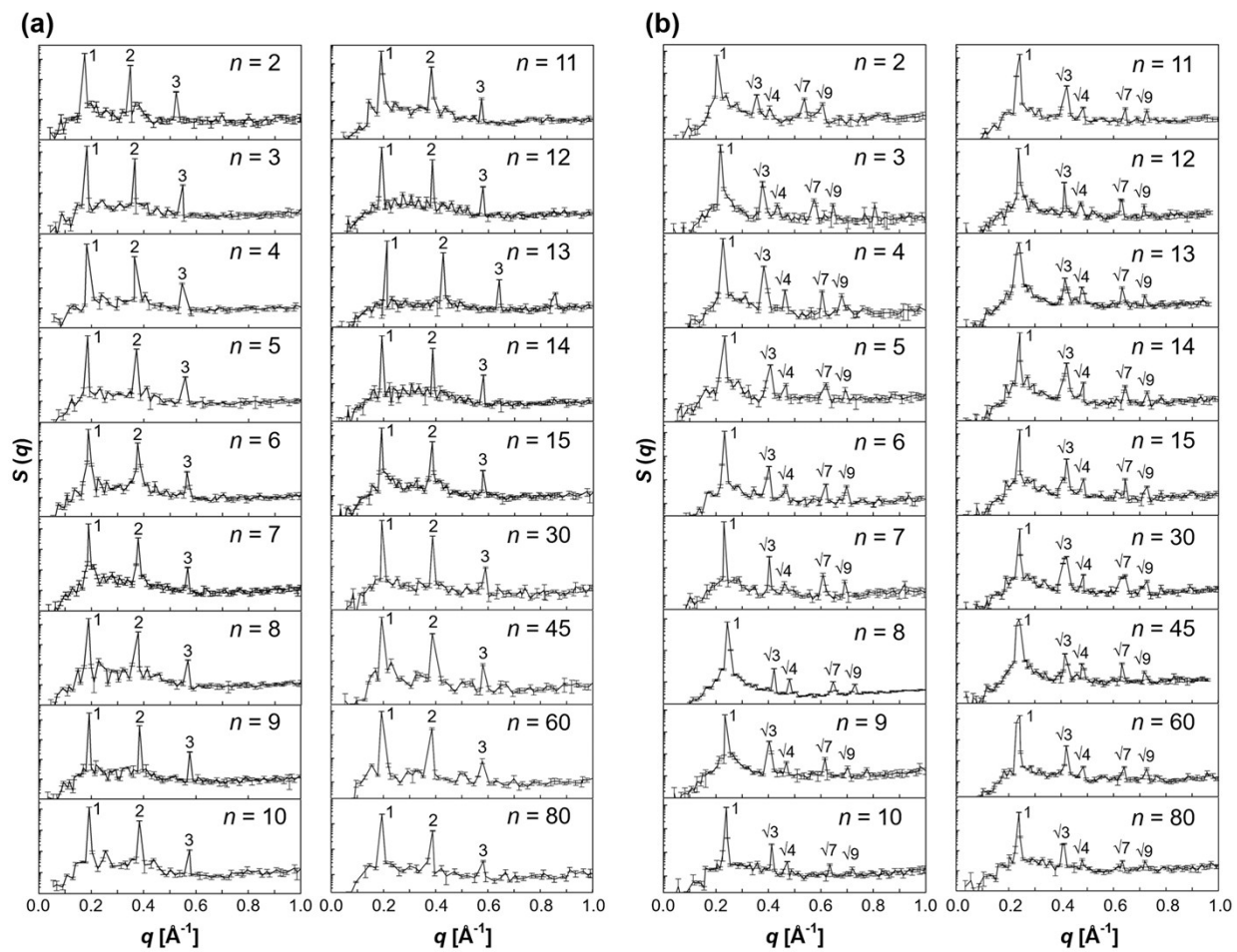


Fig. S15 Structure factors of LAM (a) and HEX (b) obtained from polymer $(A_2-C_3)_n$ and $(A_2-2C_2)_n$, where n increases from 2 to 15, 30, 45, 60 and 80.

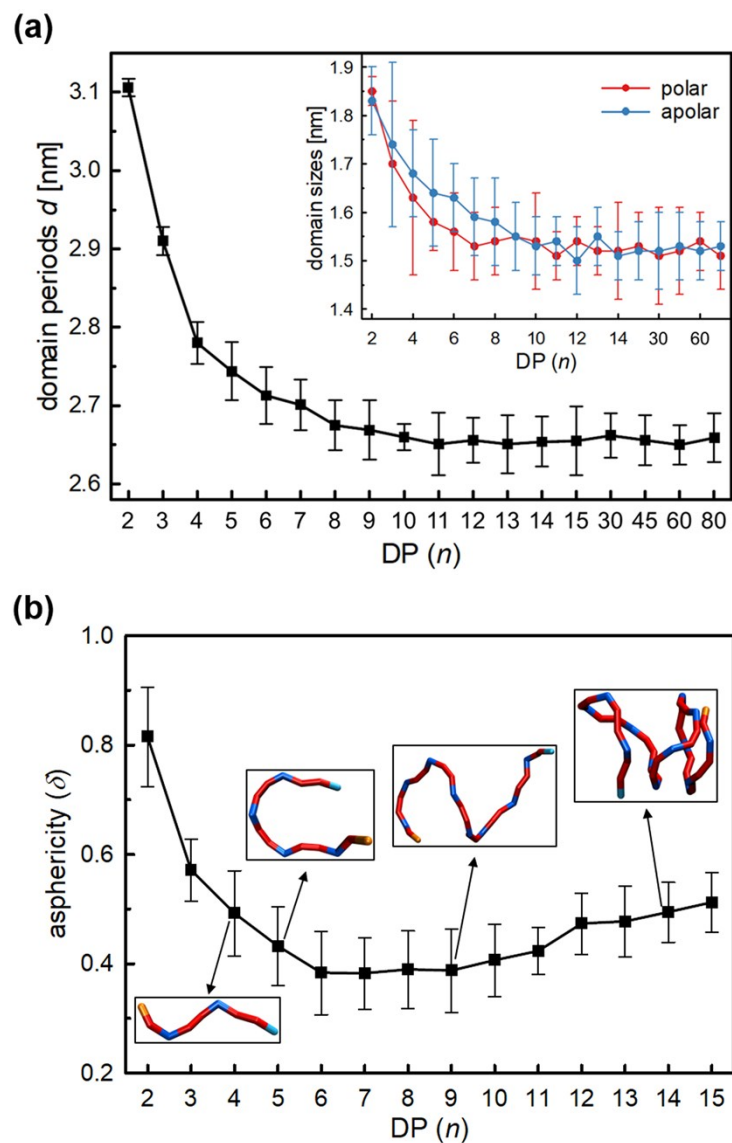


Fig. S16 (a) The variations of domain period d and the sizes of polar and apolar domains (the inset) with DP (n) for HEX obtained from polymer $(A_2-2C_2)_n$. (b) The variation of the asphericity (δ) of the polymer backbones with n . The insets show several representative conformations of polymer backbones.

S10. Glass transition temperature.

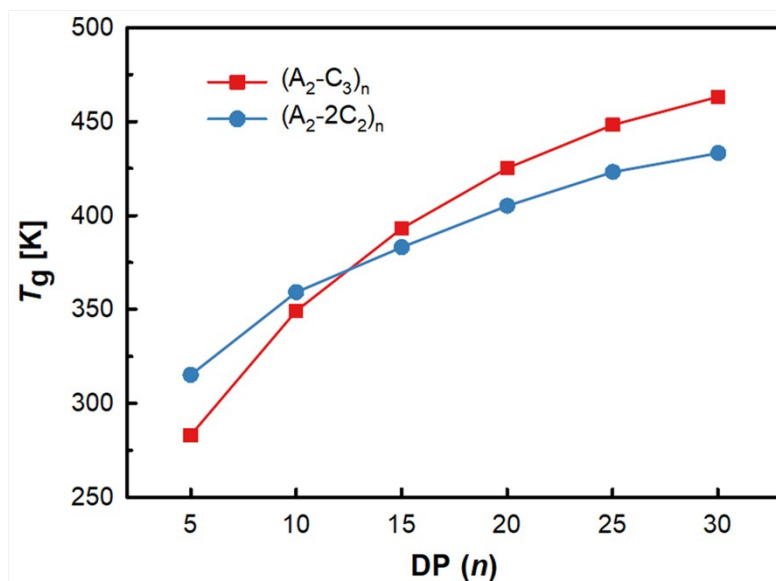


Fig. S17 The variations of glass transition temperatures (T_g) with DP (n) for polymers $(A_2-C_3)_n$ and $(A_2-2C_2)_n$.

S11. Polydisperse systems.

Table S7. The compositions of different polydisperse systems used in our simulation.

$\frac{\varphi_i}{D} \backslash n$	5	15	30	45	60	80
1.00	0%	100%	0%	0%	0%	0%
1.14	5%	10%	60%	20%	5%	0%
1.54	10%	40%	20%	10%	10%	10%
2.03	40%	30%	5%	5%	10%	15%
2.45	60%	10%	5%	5%	5%	15%
2.95	70%	10%	5%	3%	2%	10%

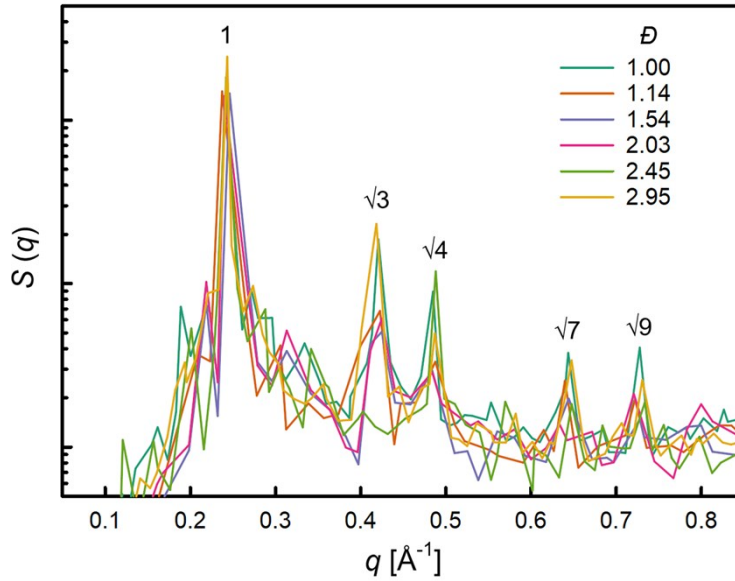


Fig. S18 Structure factors for HEX phases obtained from polymers $(A_2-2C_2)_n$ with different MWD.

References

- (1) Hansen, C. M., *Hansen Solubility Parameters-A User's Handbook*. CRC Press: Boca Raton, FL 2007.
- (2) Schultz, A. J.; Hall, C. K.; Genzer, J., Obtaining Concentration Profiles from Computer Simulation Structure Factors. *Macromolecules* **2007**, *40*, 2629-2632.
- (3) Chen, Q. P.; Barreda, L.; Oquendo, L. E.; Hillmyer, M. A.; Lodge, T. P.; Siepmann, J. I., Computational Design of High-chi Block Oligomers for Accessing 1 nm Domains. *ACS Nano* **2018**, *12*, 4351-4361.
- (4) Israelachvili, J. N., *Intermolecular and Surface Forces*. Elsevier: Amsterdam, 2011.
- (5) Theodorou, D. N.; Suter, U. W., Shape of unperturbed linear polymers: polypropylene. *Macromolecules* **1985**, *18*, 1206-1214.
- (6) Noguchi, H.; Yoshikawa, K., Morphological variation in a collapsed single homopolymer chain. *J. Chem. Phys.* **1998**, *109*, 5070-5077.
- (7) Lin, C.-M.; Chen, Y.-Z.; Sheng, Y.-J.; Tsao, H.-K., Effects of macromolecular architecture on the micellization behavior of complex block copolymers. *React. Funct. Polym.* **2009**, *69*, 539-545.